# Electronic Supplementary Information (ESI)

# Thermally rearranged (TR) bismaleimide-based network polymers for gas separation membranes†

Yu Seong Do,[‡a] Won Hee Lee,[‡a] Jong Geun Seong,[a] Ju Sung Kim,[a] Ho Hyun Wang,[a] Cara M. Doherty,[b] Anita J. Hill,[b] and Young Moo Lee*[a]

[a] *Department of Energy Engineering, College of Engineering, Hanyang University, Seoul 04763, Republic of Korea*

[b] *Commonwealth Scientific and Industrial Research Organization (CSIRO) Manufacturing, Private Bag 10, Clayton South, Victoria 3169, Australia*

*E-mail: ymlee@hanyang.ac.kr;*

† Electronic Supplementary Information (ESI) available: Detailed experimental sections and supplementary characterizations were included See DOI: 10.1039/x0xx00000x

‡ Equal contribution to this work

# 1. Materials

2,2′-bis(3-amino-4-hydroxyphenyl)-hexafluoropropane (bisAPAF) was purchased from Central Glass Co. Ltd. (Tokyo, Japan). 3,3′-dihydroxyl-4,4′-diaminobiphenyl (HAB) was purchased from Wakayama Seika Kogyo Co., Ltd. (Wakayama, Japan). Maleic anhydride (>99.0%), acetone (>99.0%), anhydrous *N*-Methyl-2-pyrrolidinone (NMP), and tetrahydrofuran (THF) were purchased from Sigma Aldrich Co. (Milwaukee, WI, USA) and used as received**.**

# 2. Synthesis and membrane fabrication

## 2.1 Synthesis of the bismaleamic acid monomer (BHMAA-6F)

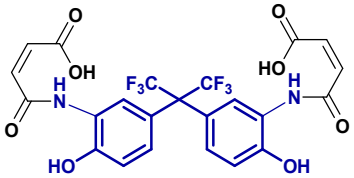


A bismaleamic acid monomer, BHMAA-6F, was prepared by a condensation reaction between maleic anhydride and bisAPAF 20 mmol of maleic anhydride was dissolved in 50 ml of acetone under an $N_2$ atmosphere and 10 mmol of APAF was added with 50 ml of acetone. The solution was stirred for 3 h. The reaction mixture was precipitated in THF, washed, and filtered off the bright yellow solid. The yellow precipitant was collected and dried at 50 °C under vacuum. Yield 59.5%; $M_p$ (Melting point) = 220 °C. $^1$H NMR (600 MHz, DMSO-$d_6$) $\delta$ 13.2 (1H), $\delta$ 10.4 (1H), $\delta$ 9.90 (1H), $\delta$ 8.09 (1H), $\delta$ 6.93 (1H), $\delta$ 6.58 (1H), $\delta$ 6.36 (1H), $\delta$ 6.32 (1H); FTIR (KBr, powder, $\nu$, cm$^{-1}$): 3314, 3092, 2254, 901, 1700, 1627, 1587, 1553, 1507, 1445, 1405, 1365, 1323, 1303, 1250, 1192, 1157, 1122, 1010, 979, 905, 888, 843, 780, 765.

## 2.2 Synthesis of the bismaleamic acid monomer (BHMAA-HAB).

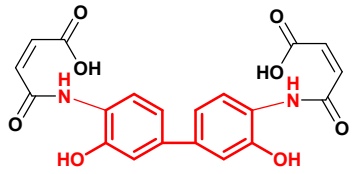


The other bismaleamic acid monomer, BHMAA-HAB, was prepared by a condensation reaction between maleic anhydride and 30 mmol of HAB, dissolved in 300 ml of acetone under an $N_2$ atmosphere. After complete dissolution, 60 mmol of maleic anhydride was added with 100 ml of acetone. The solution was stirred for 12 h. The reaction mixture was precipitated in THF, washed, and filtered off the bright red solid. The red precipitant was collected and dried at 50 °C under vacuum. Yield: 96.5%; $M_p$ (Melting point) =242 °C. $^1$H NMR (600 MHz, DMSO-$d_6$) $\delta$ 13.1 (1H), $\delta$ 10.1 (1H), $\delta$ 10.0 (1H), $\delta$ 7.92 (1H), $\delta$ 7.10 (1H), $\delta$ 6.63 (1H), $\delta$ 6.36 (1H) $\delta$ 6.34 (1H); FTIR (KBr, powder, $\nu$, cm$^{-1}$): 3390, 3159, 1870, 1813, 1694, 1630, 1600, 1559,1533, 1397, 1339, 1307, 1288, 1245, 1197, 1133, 1022, 977, 906, 868, 848, 810.

## 2.3 Bismaleimide (BMI) resin preparation

BHMAA-6F and BHMAA-HAB were dissolved in NMP and cast onto a glass plate. The casted solutions were heated to 80, 100, 120, 150, 200, and 250 °C for 1 h at each isothermal step, and the polyimide resins were formed by dehydration ring closure of amic acid groups.

## 2.4 Semi-IPN (SIPN) film preparation

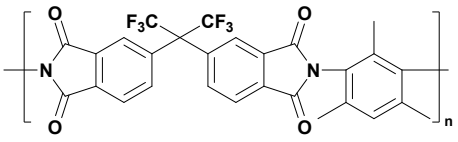

6FDA-DAM

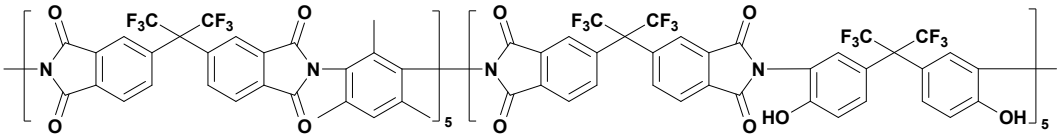

6FDA-(APAF-DAM)

**Fig. S1** Chemical structures of 6FDA-DAM and 6FDA-(APAF-DAM).

6FDA-DAM or 6FDA-(APAF-DAM) polyimide and BHMAA-6F (95/5 in weight ratio) were dissolved in NMP and cast onto a glass plate**.** The casted solutions were heated to 80, 100, 120, 150, 200, and 250 °C for 1 h at each isothermal step, and the resulting SIPN films were peeled off from the glass plate.

## 2.5 Thermal rearrangement of BMI resins

The BMI films were taken off the glass plates, rinsed with DI water, and dried *in vacuo* at 100 °C. The dried films were heated in a muffled furnace (Lenton, London, UK) to 300 °C at a rate of 5 °C/min, held for 1 h to eliminate residual solvents, heated further to 450 °C at the same speed, and maintained for 1 h under a high-purity argon atmosphere.

## 3. Characterization

Thermogravimetric analysis (TGA) with mass spectroscopy (MS) were conducted to confirm the thermal rearrangement of BHMIs with the resulting byproduct gases by TGA Q50 (TA Instruments, New Castle, DE) at a rate of 5 $^{o}$C/min from 80 $^{o}$C to 800 $^{o}$C with a ThermoStarGSD301T (Pfeiffer Vacuum GmbH, Asslar, Germany). Dynamic mechanical analysis (DMA) measurements were performed on a DMA Q800 (TA Instruments, New Castle, DE) at a rate of 5 $^{o}$C/min from 100 to 500 $^{o}$C with a load frequency of 1 Hz under a nitrogen atmosphere. Solid-state $^{13}$C NMR spectra were recorded on a Bruker Avance II spectrometer (Bruker Biospin, Rheinstetten, Germany). The attenuated total reflection Fourier transform infrared (ATR-FTIR) spectra of samples were measured using an Infrared Microspectrometer (IlluminatIR, SensIR Technologies, Danbury, CT, USA). The BET surface area and sorption characteristics were measured at 77 K by the Horvath-Kawazoe method using a surface area and porosimetry analyzer (ASAP2020, Micrometric Instruments Corp., Norcross, GA). The $CO_2$ solubility was determined using a barometric pressure decay method with a dual-volume apparatus in a closed system as previously described.[1] Positron annihilation lifetime spectroscopy (PALS) was used to determine the size of cavities within the polymer membranes using an automated EG&G Ortec (Oak Ridge, TN) fast−fast coincidence spectrometer as previously described.[2] The membranes were measured at room temperature and under vacuum (1x $10^{-6}$ Torr). A minimum of 5 files of 4.5 x $10^6$ integrated counts was collected for each membrane using a 30μCi $^{22}$NaCl source enclosed in Mylar. The average cavity size was determined from the lifetime of free positron annihilation ($\tau_2$) , described as follows:[3]

$$\tau_2 = 0.260 \times [1 - \frac{R}{R + 3.823} + \frac{1}{2\pi}\sin\left(\frac{2\pi R}{R + 3.823}\right)]^{-1}, \quad (1)$$

Where $\tau_2$ is the life time of free positron annihilation (ns) and R is the mean radius of cavities (Å). Equation 1 is valid with the mean radius of cavities up to 5 Å. [3] All of the cavity sizes in this study were expressed as diameter (*2R*) rather than radius (*R*).

Gas permeability was measured by a constant-volume (time-lag) method at 35 $^{o}$C, 1 atm for six representative gases (*i.e.,* He, $H_2$, $CO_2$, $O_2$, $N_2$ and $CH_4$). The gas permeability was determined by the rate of pressure rise under the steady-state, described as follows:

$$P = \frac{dp}{dt}\left(\frac{QT_0\, l}{AT\Delta P}\right), \quad (2)$$

where *P* is the permeability represented in Barrer (1 Barrer = $10^{-10}$·cm$^3$(STP) · cm ·cm$^{-2}$·s$^{-1}$·cmHg$^{-1}$), *dp/dt* is the rate of pressure rise under a steady state, *V* (cm$^3$) is the downstream volume, *l* (cm) is the membrane thickness, *T* (K) is the measurement temperature, Δ*P* (cmHg) is the pressure difference, *A* (cm$^2$) is the effective membrane area, and $P_0$ and $T_0$ are the standard pressure and temperature, respectively.

# 4. Analyses

## 4.1 Thermal and thermomechanical properties of BHMIs

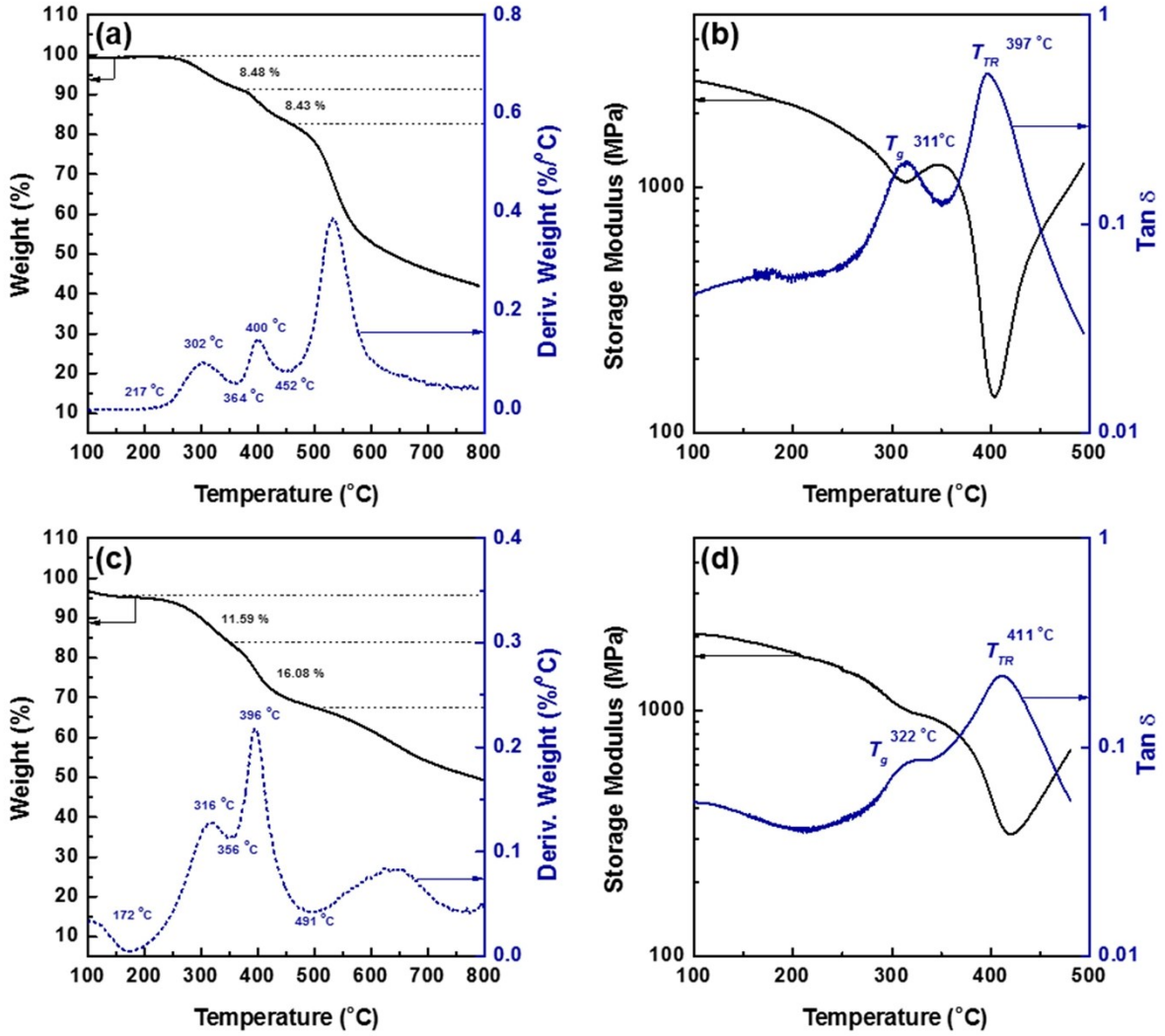


**Fig. S2** TG-MS curves of (a) BHMI-6F and (c) BHMI-HAB and DMA curves of (b) BHMI-6F and (d) BHMI-HAB.

### 4.2 Solid state $^{13}$C-NMR data of BHMI-HAB and TR-BMI-HAB

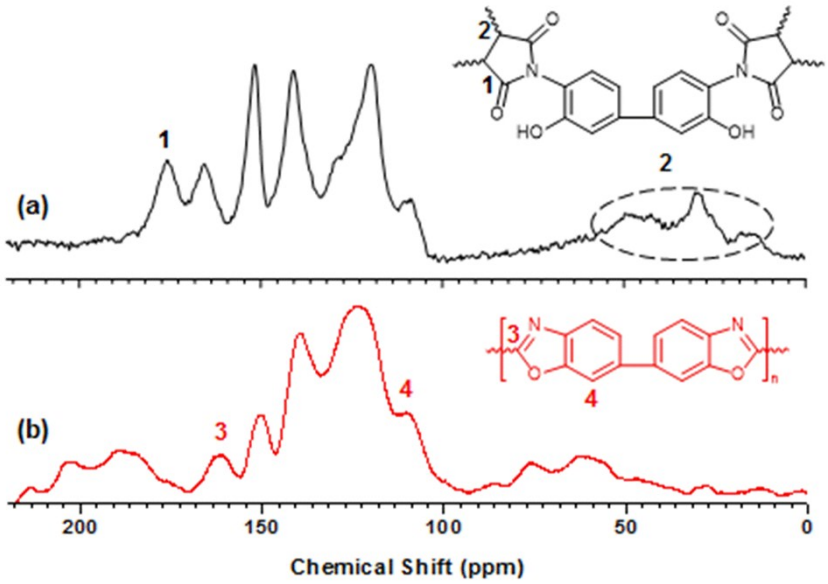


**Fig. S3** Solid-state $^{13}$C-NMR of (a) BHMI-HAB and (b) TR-BMI-HAB.

### 4.3 ATR-IR data of BHMIs and TR-BMI resins

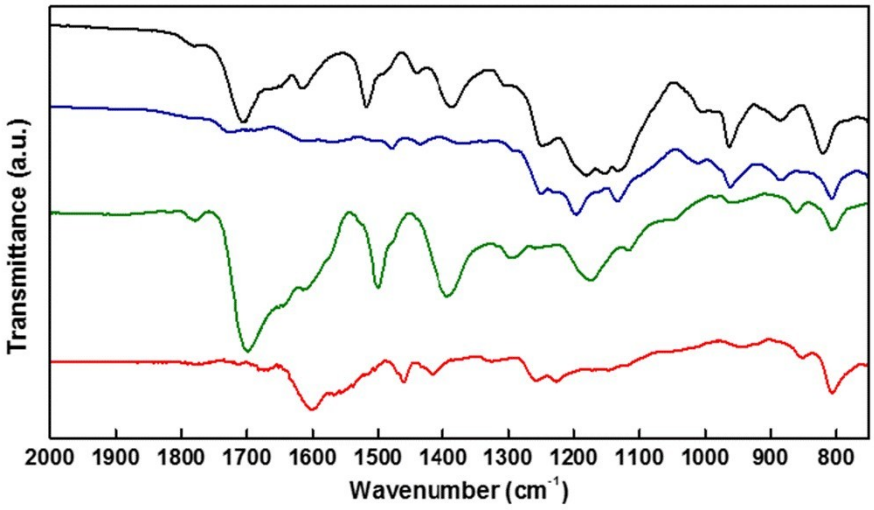

**Fig. S4** ATR-IR of BHMI-6F (— black solid), TR-BMI-6F (— blue solid), BHMI-HAB (— green solid) and TR-BMI-HAB (— red solid).

### 4.4 Nitrogen adsorption/desorption isotherms of BHMI-HAB and TR-BMI-HAB

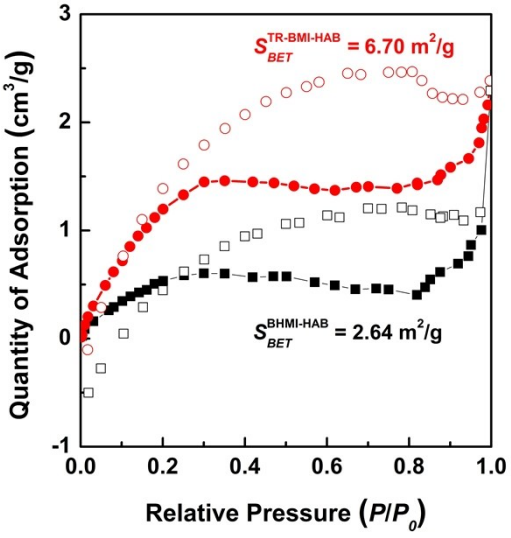


**Fig. S5** Nitrogen adsorption (solid) and desorption (dash) isotherm at 77K of BHMI-HAB (■ (black), — (solid)) and TR-BMI-HAB (● (red), — (solid)).

### 4.5 PALS Characterization

The Positron annihilation lifetime spectroscopy (PALS) spectrum for both the precursor **BHMI-6F** and resulting **TR-BMI-6F** were not observed due to the *o*-Ps inhibition effect. The *o*-Ps inhibition is quite common in some polyimides, owing to the specific chemical environment with a high electron affinity.[3] Ito et al reported that the polyimides bearing PMDA and BTDA moieties, which showed a high electron affinity, have no or little *o*-Ps component, while those bearing BPDA and 6FDA moieties, which showed a relatively low electron affinity, exhibited substantial *o*-Ps formation.[4] In this work, **BHMI-6F** and **TR-BMI-6F** are originated from the maleic anhydride derivatives, a representative functional group with a high electron affinity, which frustrates to calculate cavity size distribution based on the *o*-Ps annihilation ($\tau_3$). Instead, the average pore size based on the lifetime of free positron annihilation ($\tau_2$) are available as shown in Table S1

**Table S1.** PALS Characterization of Cavity Size in BHMI-6F and TR-BMI-6F.

| Polymer | $\tau_2$ (ns) | Cavity Diameter (Å) |
|---|---|---|
| **BHMI-6F** | 0.387 ± 0.003 | 5.36 ± 0.08 |
| **TR-BMI-6F** | 0.413 ± 0.002 | 5.87 ± 0.04 |

## 4.6 Gas transport properties

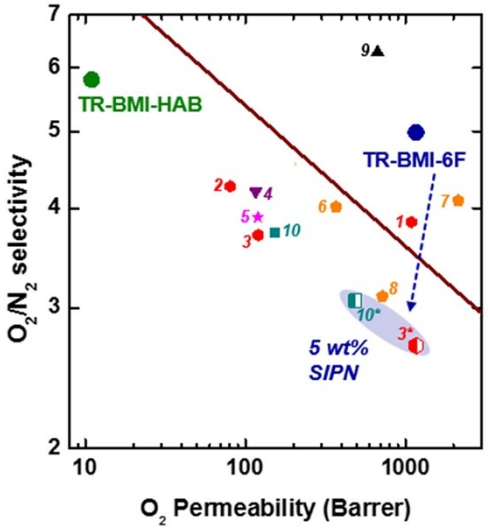


**Fig. S6** Robeson plots of corresponding TR-BMI resins for the $O_2/N_2$ gas pair (solid lines represent the 2008 upper bound). Data points are from reported TR polymers (red), PIMs (orange), KAUST-PI (black), crosslinked TR polymers (purple) and spirobisindane-containing TR-PBO (magenta) for comparison. The representative data points are as follows: (1) tPBO;[2] (2) aPBO;[2] (3) 6FDA-(APAF+DAM); (3') 6FDA-(APAF+DAM) SIPN with 5wt% TR-BMI-6F; (4) XTR-PBOI-5;[5] (5) SpiroPBO-6F;[6] (6) PIM-1;[7] (7) PIM-EA-TB;[8] (8) PIM-SBI-TB;[8] (9) KAUST-PI-1;[9] (10) 6FDA-DAM ; (10') 6FDA-DAM SIPN with 5wt% TR-BMI-6F.

**Table S2.** Single gas permeability (*P*) and ideal selectivity for BHMI and SIPN membranes

| Polymer | Permeability (Barrer) | | | | | | Ideal selectivity (α) | | | | | |
|---|---|---|---|---|---|---|---|---|---|---|---|---|
| | He | $H_2$ | $CO_2$ | $O_2$ | $N_2$ | $CH_4$ | $H_2/CO_2$ | $O_2/N_2$ | $CO_2/N_2$ | $H_2/N_2$ | $H_2/CH_4$ | $CO_2/CH_4$ |
| ***Precursors*** | | | | | | | | | | | | |
| **BHMI-6F** | 18 | 9.7 | 1.6 | 0.46 | 0.07 | 0.02 | 6.0 | 7.0 | 25 | 150 | 445 | 74 |
| **BHMI-HAB** | 3.21 | 2.08 | 0.24 | *NA* | *NA* | *NA* | 8.66 | *NA* | *NA* | *NA* | *NA* | *NA* |
| **6FDA-DAM** | 399 | 553 | 524 | 101 | 25 | 16 | 1.1 | 4.0 | 21 | 22 | 35 | 33 |
| **6FDA-(APAF+DAM)** | 86 | 74 | 43 | 8.9 | 1.8 | 1.0 | 1.7 | 4.9 | 23 | 40 | 73 | 42 |
| **6FDA-DAM** ***+ 5 wt% BHMI-6F*** | 261 | 351 | 372 | 69 | 19 | 14 | 0.94 | 3.6 | 20 | 18 | 25 | 27 |
| **6FDA-(APAF+DAM)** ***+ 5 wt% BHMI-6F*** | 69 | 57 | 31 | 6.4 | 1.3 | 0.74 | 1.8 | 4.9 | 24 | 44 | 77 | 42 |
| ***450 °C Thermal treatment*** | | | | | | | | | | | | |
| **TR-BMI-6F** | 2139 | 5122 | 5440 | 1171 | 235 | 145 | 0.9 | 5.0 | 23 | 22 | 35 | 37 |
| **TR-BMI-HAB** | 59 | 99 | 57 | 11 | 1.9 | 1.7 | 1.7 | 5.57 | 30 | 52 | 58 | 33 |
| **6FDA-DAM** | 383 | 635 | 803 | 153 | 41 | 39 | 0.79 | 3.7 | 20 | 15 | 16 | 21 |
| **6FDA-(APAF+DAM)** | 419 | 554 | 595 | 121 | 33 | 24 | 0.93 | 3.7 | 18 | 17 | 23 | 25 |
| **6FDA-DAM** ***+ 5 wt% TR-BMI-6F*** | 771 | 1514 | 2706 | 487 | 159 | 161 | 0.56 | 3.1 | 17 | 10 | 9.4 | 17 |
| **6FDA-(APAF+DAM)** ***+ 5 wt% TR-BMI-6F*** | 1496 | 3072 | 6149 | 1169 | 434 | 446 | 0.50 | 2.7 | 14 | 7.1 | 6.9 | 14 |

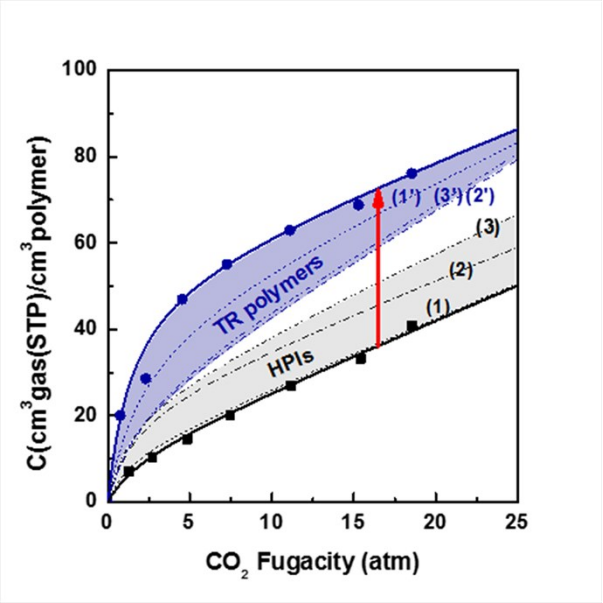


**Fig. S7** $CO_2$ sorption isotherms at 35 °C of BHMI-6F (● (black), — (solid)) and TR-BMI-6F (● (blue), — (solid)). Other TR polymers are used for comparison: (1) tHPI (-- (black short dash)), (2) aHPI (-·- (black dash dot)), (3) cHPI (-···- (black dash dot dot)), (1') tPBO (-- (blue short dash)), (2') aPBO (-·- (blue dash dot)), (3') cPBO (-···- (blue dash dot dot)). [2] All of lines are provided to guide the eye.

## References


1 J. G. Seong, Y. Zhuang, S. Kim, Y. S. Do, W. H. Lee, M. D. Guiver and Y. M. Lee, *Journal of Membrane Science*, 2015, **480**, 104-114.

2 S. H. Han, N. Misdan, S. Kim, C. M. Doherty, A. J. Hill and Y. M. Lee, *Macromolecules*, 2010, **43**, 7657-7667.

3 K.-S. Liao, H. Chen, S. Awad, J.-P. Yuan, W.-S. Hung, K.-R. Lee, J.-Y. Lai, C.-C. Hu and Y. Jean, *Macromolecules*, 2011, **44**, 6818-6826.

4 Y. Ito, K.-I. Okamoto and K. Tanaka, *Le Journal de Physique IV*, 1993, **3**, C4-241-C244-247.

5 M. Calle, H. J. Jo, C. M. Doherty, A. J. Hill and Y. M. Lee, *Macromolecules*, 2015, **48**, 2603-2613.

6 S. Li, H. J. Jo, S. H. Han, C. H. Park, S. Kim, P. M. Budd and Y. M. Lee, *Journal of Membrane Science*, 2013, **434**, 137-147.

7 P. Budd, K. Msayib, C. Tattershall, B. Ghanem, K. Reynolds, N. McKeown and D. Fritsch, *Journal of Membrane Science*, 2005, **251**, 263-269.

8 M. Carta, R. Malpass-Evans, M. Croad, Y. Rogan, J. C. Jansen, P. Bernardo, F. Bazzarelli and N. B. McKeown, *Science*, 2013, **339**, 303-307.

9 B. S. Ghanem, R. Swaidan, E. Litwiller and I. Pinnau, *Advanced materials*, 2014, **26**, 3688-3692.